Hindawi
Journal of Electrical and Computer Engineering
Volume 2023, Article ID 8527308, 19 pages
https://doi.org/10.1155/2023/8527308

Research Article

Power System Analysis of Moving from HVAC to HVDC in the Presence of Renewable Energy Resources

Osama Saadeh, Baher Abu Sba, and Zakariya Dalala

Energy Engineering Department, German Jordanian University, Amman 11180, Jordan

Correspondence should be addressed to Osama Saadeh; osama.saadeh@gju.edu.jo

Received 22 March 2023; Revised 15 October 2023; Accepted 26 October 2023; Published 8 November 2023

Academic Editor: Rossano Musca

As global energy consumption continues to increase, increased utilization and adaptation of renewable energy resources have tremendously increased over the last decades. Unfortunately, despite the many benefits of renewable energy resources, the intermittent nature of generation and the far distance of large installations from demand centers have tremendous effects on the connecting grid's stability. In this study, high-voltage direct current (HVDC) systems are proposed as a solution for stable and reliable grid operation in the presence of large renewable energy installations. This research investigates the deployment of an HVDC system into an entire network rather than studying it as an isolated radial system. Various power system analysis functions for both static and dynamic conditions are used to study the effect of integrating an HVDC system on the overall network's stability. To verify the proposed approach, Jordan's national electric grid was modeled and used as a case study. The results show when deploying HVDC transmission, losses are reduced by 70% from the baseline case, in addition to better handling of contingency events and enhanced grid's stability when examining the generator's rotor angle and speed. Rigorous modeling and simulations of the proposed system structure show the feasibility and prove the advantages of modern HVDC systems over HVAC counterparts.

1. Introduction

High-voltage alternating current (HVAC) transmission systems have been deployed for decades, as they reduce system losses and increase transmission efficiency. However, HVAC systems are facing several challenges and issues due to increased renewable energy penetration and long-distance power transmission. The main challenges include reduced transmission power capacity, limited transmission distance, increased reactive power losses, stability issues under faults and transient conditions, and transmission line inductive and capacitive voltage regulation issues. In addition, stability-induced complications can limit network interconnections and expansion [1]. Moreover, HVAC system operation requires a considerable amount of reactive power generation, which increases the current, leading to increased transmission losses. The noncontrollable nature of renewable energy generation impacts traditional generation spinning reserves to balance system-wide generation with load demand which affects system adequacy and security [2]. It is worth noting that the development of power transmission infrastructure is significantly impacted by socio-environmental issues and the widespread use of HVAC overhead lines has been hampered by community opposition and environmental concerns.

Alternatives for increasing power transfer capability are needed to overcome the challenges described above [3]. In addition, the construction of new lines may be restricted by right-of-way (ROW) or environmental constraints and high cost.

High-voltage direct current (HVDC) transmission systems are an attractive alternative to mitigate the many issues HVAC systems face. In the past, HVDC transmission faced obstacles, mainly due to low voltage DC generation and no efficient transformer alternative, leading to short-distance transmission. With advances in power electronics [4–6], the efficient step-up of DC voltage has been made possible, leading to HVDC systems that are capable of long-distance

transmission. As power electronic circuits and devices continue to mature, the benefits of adopting DC systems will continue to increase.

An HVDC transmission system may exist between AC generation and AC load. It includes an AC/DC converter station at the sending terminal, known as a rectifier, and a DC/AC converter station at the receiving terminal, known as an inverter, with the HVDC transmission line in between for unidirectional operation. Bidirectional converters may also be deployed for a two-way operation. The connection point between the AC and DC systems is called the point of common coupling (PCC). It is typically used to track and control the active and reactive power injection into and out of the AC system [7]. Two different types of converter stations are typically used: line-commutated converters (LCC) and voltage source converters (VSC). Both of these may be applied in various configurations such as monopolar and bipolar connections [8–10]. The converter in LCC-HVDC systems is based on thyristors, which are turn-on switches. For thyristors, gate control signals are used to control the operation mode depending on the firing angles. For a rectifier, the firing angles, or ignition angle, should be between 0 and 90 degrees, whereas for an inverter, the firing angles should be between 90 and 180 degrees [11]. VSC-HVDC technology is newer than LCC-HVDC and it has been improving significantly. The converter in VSC-HVDC systems is based on self-commutating switches, which turn on/off, such as gate turn-off thyristors (GTOs) and insulated-gate bipolar transistors (IGBTs). VSCs use the pulse-width modulation (PWM) technique and operate at a high frequency to control the gate-switching frequency [9]. VSC-HVDC systems have the ability to switch the current on and off at any time, regardless of the AC voltage; in reality, they recover from blackout cases by generating their own AC voltage. The active and reactive powers are controlled separately. It has the advantage of providing reactive power to support the system's stability [12]. Converter stations are the most expensive HVDC component, which is the main challenge of HVDC deployment.

Even though HVDC systems require high-priced converter stations, this is a fixed initial cost and is offset by the lower operating cost. Nevertheless, HVDC may not be financially feasible for short distances [11]. The break-even distance is the point where the HVDC system becomes more economically feasible than HVAC. There are different estimated ranges for HVDC break-even distance. Typically, break-even distances range from 300 to 800 km for overhead lines, and from 50 to 100 km for underground cables, depending on route-specific conditions such as local policies, ROW, transmission lines installation costs, and power and voltage ratings [11, 13, 14].

Moreover, due to grid stability drawbacks, more AC lines are often needed to transmit the same amount of power over the same distance than DC lines. In addition, long-distance AC lines generally require intermediate switching stations and reactive power compensation [11, 15].

Deployment of HVDC transmission systems is growing in some applications that can benefit from their many advantages, such as stability and robustness compared to existing HVAC systems [16]. Also, HVDC outperforms HVAC transmission systems by reducing fault currents, having less corona effect, lower radio interferences, sharing utility ROW without reducing reliability, mitigating environmental issues, economics of long-distance bulk power transmission, and controllability [10, 17]. Furthermore, the higher voltage in HVDC transmission helps overcome the transmission line's voltage drop and stability limits [18]. HVDC is more flexible in power exchange than HVAC; it has a faster control of power flow and is independent of other parameters such as frequency and voltage [1]. Despite the fact that HVDC systems, especially VSC-HVDC, have advanced significantly, it is important to acknowledge the continued need for thorough studies and investigations focusing on the reliability of VSC-HVDC cables and lines and AC/DC converters, where the accuracy of the VSC-HVDC models can be affected by the choice of cable model [19].

HVDC transmission systems increase the transmission capacity and reduce power losses through the line. The capacity may increase by a factor of 3.5 of HVAC systems when using the same size transmission lines, and keeping the mechanical performance of the towers, including the body and foundations, largely unchanged [20, 21]. The conversion from HVAC overhead lines to HVDC offers environmental benefits, increased power capacity, and economic advantages for specific scenarios. By considering case studies, priority can be given to congested transmission lines requiring a substantial capacity boost while minimizing right-of-way challenges and permitting procedures [22, 23].

Although HVAC does have advantages over HVDC, such as lower installation costs, HVDC is a more efficient solution, and it may prove feasible over the system's lifetime.

The main cable losses in HVDC are limited to resistive losses due to the absence of capacitive and inductive charging effects, and the power factor is unity throughout the DC system. Also, there is no skin effect in HVDC lines, which increases the rated current due to lower cable resistance than in HVAC lines [24]. The largest share of the total losses in HVDC systems is found in the converter stations; in contrast, the significant losses in HVAC systems are cable losses [12].

Several studies investigated the HVDC transmission system's performance and compared it with HVAC transmission. In [25], researchers evaluated both LCC-HVDC and VSC-HVDC transmission systems, as well as their operating characteristics, power rating capability, control capability, and power losses. In addition, the transient response to faults in the AC side at both HVDC ends was examined. It was shown that the converter's controllers contribute to reduce the impact of faults at the converter, proving the HVDC systems' immunity to AC faults. The study is based on an HVDC link installed between two external AC grids. The design only considered a point-to-point HVDC link without considering any external HVAC line or the overall grid's performance.

The effect of replacing a single 400 kV HVAC overhead line with LCC-HVDC and VSC-HVDC transmission systems on the grid is examined in reference [1], with the

presence of high renewable energy sources (RES) generation. It was noted that the LCC-HVDC transmission systems require reactive power compensators; whereas, in the VSC-HVDC transmission system, the reactive power can be controlled independently, improving voltage stability.

In [26], two large generation sources are shared for the IEEE-RTS system and IEEE-39-bus system in the presence of large renewable energy generation with different generation mix ratios. Interconnection between the two systems is used to show the benefits of HVDC transmission. Results showed that the HVAC grid needs to generate a higher capacity than the HVDC grid to compensate for the power losses. Moreover, AC interconnection needs more parallel lines. The proposal to install a new HVAC power path is also discussed in reference [27].

Authors in reference [28] proved that installing HVDC lines in parallel with existing HVAC might be a solution for the transmission capacity since constructing new overhead lines can be problematic. It is also shown in reference [29] that integrating an HVDC transmission system improves the power flow through the higher capacity of the HVDC transmission system and voltage assistance, thus reducing system operating costs.

In [30], a VSC-HVDC transmission system is proposed to link two areas in Pakistan. The economic analysis demonstrated that the proposed system would provide economic stability and energy security to the region.

The literature also examines the effect of HVDC transmission across international borders [31–34]. This is indeed an interesting topic but only looks at the internal national grids as a lumped system, without considering the internal dynamics which are investigated in this work. Furthermore, some studies have specifically explored the impact of embedded HVDC, particularly for VSC-HVDC, on the overall system [35].

A comprehensive evaluation analysis is needed to examine the overall grid performance under steady-state and transient conditions in the presence of extensive renewable energy penetration. This study incorporates the HVDC system into an entire network rather than analyzing it as an isolated radial system. The analyses will consider different scenarios in both static and dynamic states in the presence of high-RES generation. The overall system response will be evaluated rather than focusing only on the HVDC link. This is a gap in the literature, where only the HVDC system is typically studied. In this paper, the replaced transmission system, in addition to the entire network, is examined. The analysis and studies used are explained in detail in the next section. Jordan's national electric network will be modeled and taken as a case study to examine the HVDC transmission system using a realistic network.

A complete power system analysis of all parts of the grid must be completed in order to evaluate the effect of HVDC integration. As can be observed from the literature, this has not been performed and is the focus of this work.

In this paper, Section 2 details the methodology used. Section 3 provides the modeling approach, explaining the aggregated systems' methodology and the Jordan's national electric system model. Section 4 offers insight into the DIgSILENT PowerFactory model, while Section 5 presents the simulation results and discussion, which are followed by the conclusion in Section 6.

2. Methodology

The main scope of this research is to investigate the grid's overall performance in the presence of RES. A systematic approach is proposed that evaluates the important system stability considerations through standardized, well-defined power system stability analysis for static and dynamic conditions.

Load flow, sometimes called power flow, is a fundamental analysis to investigate the system during steady-state conditions, ensuring that generation equals the sum of demand and losses, and verifies that the voltage of each busbar is close to rated values. Active and reactive power, node voltage magnitudes and angles, transmission line losses, and loadings can all be found using this method. The dispatched load flow approach is used in this research, which means that the active power balance is formed by a single reference generator or an external grid, known as the slack bus. Nevertheless, a distributed slack approach on the synchronous generators can be used to balance the active power.

Since power systems should deliver power reliably and safely, adequate short-circuit handling must be considered. Consequently, the systems' behavior under short circuit or fault event should be studied using the short-circuit analysis method. There are several standards for short-circuit calculations, for example, VDE0120, ANSI/IEEE 946, IEC61363, and IEC60909 [36–39]. However, a complete method, or a superposition method, is used in this research based on the precise evaluation of the fault current. In fact, the complete method is not a calculation performed under any particular standard; it is based on a more comprehensive set of data than the simplified calculations used by standards. Therefore, it produces more accurate results for initial short-circuit currents. Furthermore, the complete method considers the current flowing from the loads and RES in the network, whereas in IEC 60909, for example, the load currents are neglected during calculations. Accordingly, the IEC 60909 is helpful for the design stage of a project, while the complete method helps analyze projects during operation [40, 41].

Contingency analysis investigates power flow changes due to a generator, transmission line, or transformer outages [42]. It is used to assess the system's stability after unplanned events or outages for a single element (N-1) or a group of elements (N-k). Several violations could occur from outages, such as a sudden voltage rise or drop, exceeding transmission line loading limits, or overloading in some branches, which may lead to stability issues. Contingency analysis results are used to predict the issues caused by the outages and help develop strategies to overcome them [43, 44].

The root mean square (RMS) simulation is used to investigate system dynamics during transient events in both balanced and unbalanced conditions. It is used in many applications, such as studying the compliance of RES or

HVDC systems design. Many events can be studied using this tool, especially short-circuit events, switching events, and outages of an element. However, this analysis is mainly used in this research to investigate the synchronous generator's rotor angle stability to determine the critical clearing time (CCT). The procedure for this analysis is illustrated in Figure 1.

The short-circuit events are utilized using IEEE Std. 3002.3, which implies that the short-circuit event is applied using a bolted three-phase short-circuit with a duration of 1.5–4 cycles, i.e., 0.03–0.08 seconds at 50 Hz [45]. The event definition method is explained in Figure 2, where $t_2 = t_1 + 0.08$ as per the standard.

Jordan's national electric grid will be modeled in DIgSILENT PowerFactory software and a single HVAC line will be replaced with an HVDC system. The methodology that will be used in the study is as follows: to analyze simulation results and compare the outcome of the original HVAC model with both the LCC-HVDC and VSC-HVDC systems, using the power system analysis described above. The models used are all standard software models that have been extensively used in the literature. Thus, even though power system models are generally not verified against real event data, emulating such scenarios realistically is not possible; the models are adherently sound and accepted by the research community. All models have been characterized using actual data from official sources and reports, thus the results can be considered accurate within an acceptable range.

3. Modeling Approach

To better model the electric grid in this research, the network will be divided into several connected aggregated systems. As the focus of the study is the transmission system, details within the distribution system are insignificant, and thus lumped into one node. All the characteristics related to load and generation are still captured, which still allows for accurate grid-wide analysis. Abstracting and simplifying parts of the grid will better demonstrate and highlight the results. Boundaries and assumptions will also be defined.

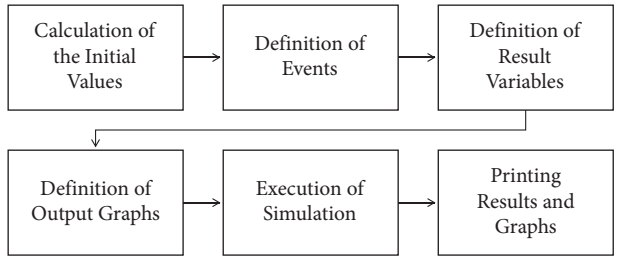

Figure 1: RMS simulation procedure.

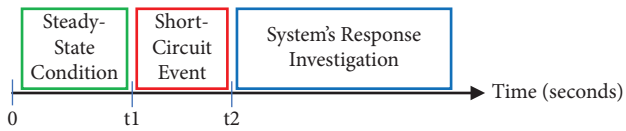

Figure 2: RMS events definition.

3.1. Aggregated Systems. The electrical grid is abstracted into three levels: load, transmission, and generation. The aggregated system is the abstraction of the system for a particular geographical part of the network, for example, northern, central, and southern areas.

The study's focal point is on the transmission level. Hence, the transmission voltages in the study are 132 kV and 400 kV, which are the actual transmission voltages in Jordan. While the 33 kV distribution level is considered as part of the system's load.

The load data, which are usually provided as an annual demand in GWh, are not adequate for modeling. The load distribution approach must consider the load factor (LDF), which indicates the average load from the load curve. The load factor value is usually less than or equal to one and is calculated by using equation (1) [46].

$$\text{LDF} = \frac{\text{Average Demand (MW)}}{\text{Peak Demand (MW)}} \times 100\%. \quad (1)$$

The average demand in MW is found by using equation (2). The load distribution approach requires the diversity factor (DF), expressed in equation (3) [47].

$$\text{Average Demand (MW)} = \frac{\text{Total Energy (GWh)}}{\text{Total Period (hours)}} \times \frac{1000\text{MW}}{1\text{GW}}, \quad (2)$$

$$\text{DF} = \frac{\sum(\text{Individual Maximum Demands})}{\text{Maximum Demand of the System}}. \quad (3)$$

Each aggregated system has two substations, 400/132 kV and 132/33 kV, and each substation is designed with two parallel transformers. Therefore, the substation ratings are calculated as shown in equation (4) and to account for future expansion, a 30% percent safety margin is used as an acceptable market practice.

$$\text{Subsation Rating (MVA)} = \text{Total Generation in Aggregated System (MVA)} \times 1.3. \quad (4)$$

The aggregated systems are connected with double-circuit overhead lines. Their specifications depend on the actual installed transmission line, where the rated current is calculated by using equation (5).

$$I_{\text{rated}} = \frac{S_{\text{rated }3\varnothing}}{\sqrt{3} \times V_{\text{rated}L-L}}. \quad (5)$$

3.2. Jordan's National Electric System Model. Jordan's national electrical grid is used as a case study. The system's boundaries are taken as the countries' borders and the connected neighboring countries are not considered in this model.

In Jordan, most of the RES is in the southern part of the country (the city of Ma'an), and most of the electrical demand is located in the central region (the city of Amman). Therefore, long-distance power transmission is needed. The National Electric Power Company (NEPCO) is the authority responsible for electric power transmission in Jordan. The transmitted power by NEPCO is delivered to the three distribution companies, which are the Electricity Distribution Company (EDCO), Jordanian Electric Power Company (JEPCO), and Irbid District Electricity Company (IDECO).

The main scope of this study is the "Green Corridor," which transmits generated power from the southern part of the country to the central area. This transmission line will be switched to HVDC in this study. Therefore, Jordan's grid is abstracted into four aggregated systems: Aqaba, Ma'an, Qatrana, and "Amman and North," as shown in Figure 3. The geographical locations for the aggregated systems with their center locations are illustrated in Figure 4. Actual transmission line, load, and substation information was obtained from the different electric companies[48, 49].

Since the power plants and loads are distributed around the country, they are assigned between the aggregated systems based on their geographical locations. The aggregated systems' generation units are shown in Table 1, where renewable energy generation is shown for both photovoltaic (PV) and wind [50].

The annual consumption for the three distribution companies in 2019 was 3443.5 GWh, 11230.1 GWh, and 3680.3 GWh for IDECO, JEPCO, and EDCO, respectively [51]. All loads for IDECO and JEPCO are in the "Amman and North" aggregated system whereas EDCO loads will be divided among the aggregated systems as follows: Aqaba's load within the Aqaba aggregated system, Ma'an's and Tafila's loads in Ma'an's aggregated system, Karak's load in the Qatrana aggregated system, and Jordan Valley's load in the "Amman and North" aggregated system. The pie chart in Figure 5 shows the distribution of customers in EDCO [48].

The loads in the system are diversified, as the number of customers includes different types of consumption. Consequently, the loads are divided based on the consumption for each individual city instead of taking the number of customers. Based on the available data from 2019, the total consumption over a year for EDCO regions is tabulated in Table 2.

The peak load in Jordan in 2019 was 3380 MW [51]. Therefore, the LDF for the Jordanian system is 62%, which means the average demand is 62% of the peak demand. Furthermore, the DF is 1.03, reflecting that the load is slightly diversified as most of it is concentrated in Jordan's central area. The total loads in Jordan's aggregated systems are summarized in Table 3. A power factor of 0.95 inductive is selected for all loads.

The transmission line data provided by NEPCO are tabulated in Table 4, where all transmission lines in the system are double-circuit lines.

4. DIgSILENT PowerFactory Model

The DIgSILENT® PowerFactory 2021 SP5 simulation program is used for modeling and simulation in this study. This software was chosen for its capability in analyzing generation, transmission, and distribution systems under static and dynamic conditions [52]. In addition, this software has the capability to include power electronics equipment in the power system simulation. Since DIgSILENT PowerFactory uses a single database for all equipment in a power system, it can efficiently execute all power simulation functions within a single program environment. Investigations and comparisons will be based on standard analyses with different scenarios. The software has been widely used in the literature, as in [25, 53–55].

Jordan's network was chosen as a case study and the single-line diagram (SLD) is shown in Figure 6. Ma'an aggregated system has the most RES generation, while the "Amman and North" aggregated system has the largest demand. The "Green Corridor" is the transmission line connecting the two, which is the primary target of this study.

The Green Corridor is investigated in three different cases: HVAC, LCC-HVDC, and VSC-HVDC transmission. Each of these is modeled by adapting the existing HVAC without changing the transmission line, as shown in the following subsections.

4.1. Jordan's Model Using the HVAC Transmission System. The existing system uses an HVAC transmission system, as can be seen in Figure 6. It will be investigated and compared with the proposed HVDC transmission systems, where the target line is the Green Corridor (Ma'an–Qatrana's 400 kV overhead line).

4.2. Jordan's Model Using the LCC-HVDC Transmission System. The Green Corridor is changed to a bipolar LCC-HVDC transmission system and it transmits power from Ma'an to Qatrana. Accordingly, the rectifier station is installed at the Ma'an 400 kV busbar, where the inverter station is installed at the Qatrana 400 kV busbar to maintain the same power flow, as illustrated in Figure 7.

The converter stations' transformers have a unity nominal turns ratio to demonstrate the voltage level difference between AC and DC systems. The DC voltage of the ideal uncontrolled converter can be found by using equation (6) [40].

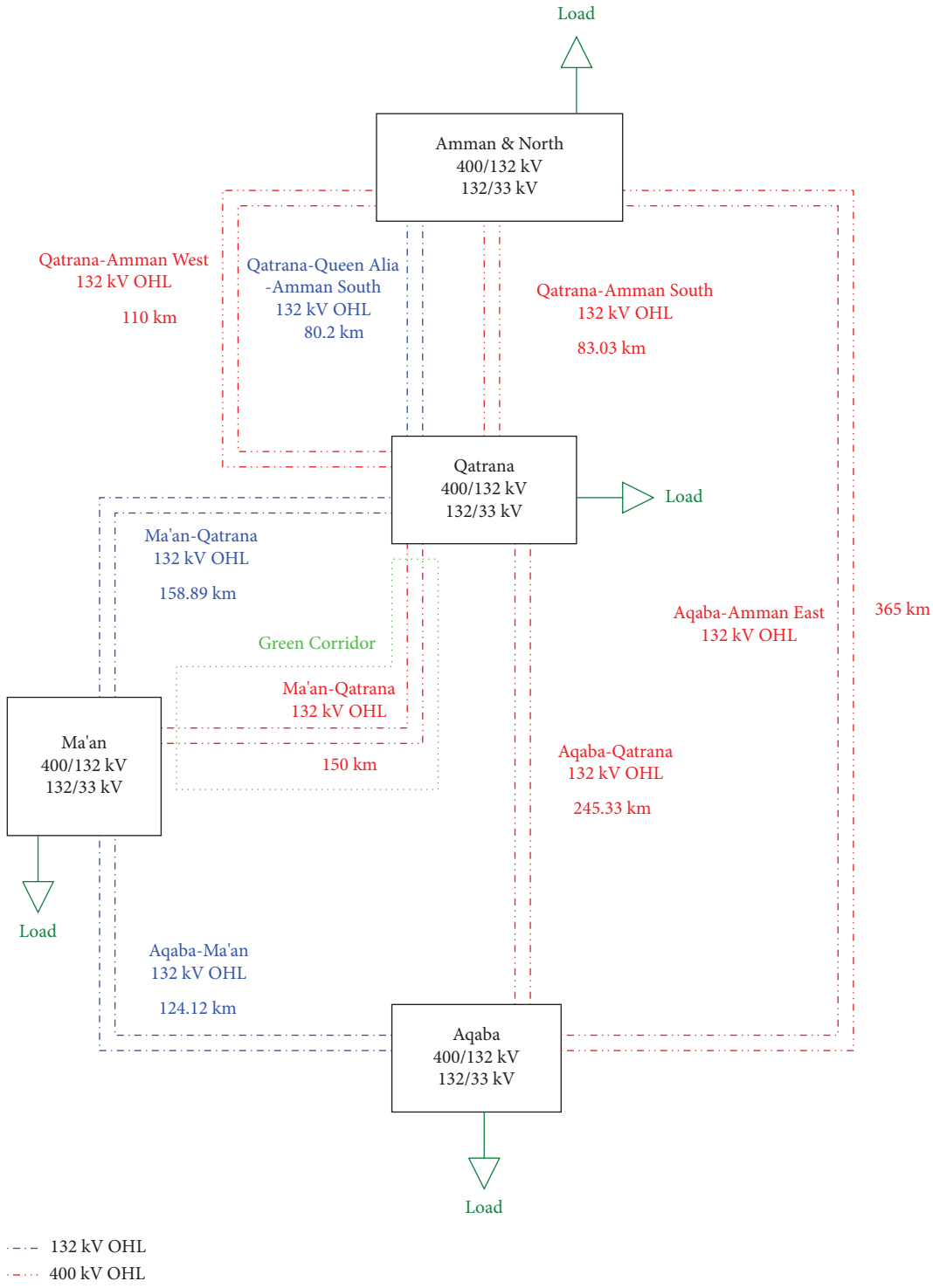

Figure 3: Aggregated systems block diagram.

$$U_{d0} = \frac{s_0 \times q}{\pi} \times \sin\left(\frac{\pi}{q}\right) \times \frac{\sqrt{2}}{\sqrt{3}} \times U_{L-L}, \quad (6)$$

where s_o defines the number of commutation groups, q is the number of branches in a commutation group, and U_{L-L} is the AC voltage supplied to the converter station. The converters are 6-pulse converters, where there are two commutation groups and three branches in each group. Accordingly, the DC voltage is calculated by using equation (7).

$$U_{d0} = \frac{3 \cdot \sqrt{2}}{\pi} \cdot U_{\mathrm{LL}} \approx 1.35 U_{\mathrm{LL}} = 540.19 kV. \quad (7)$$

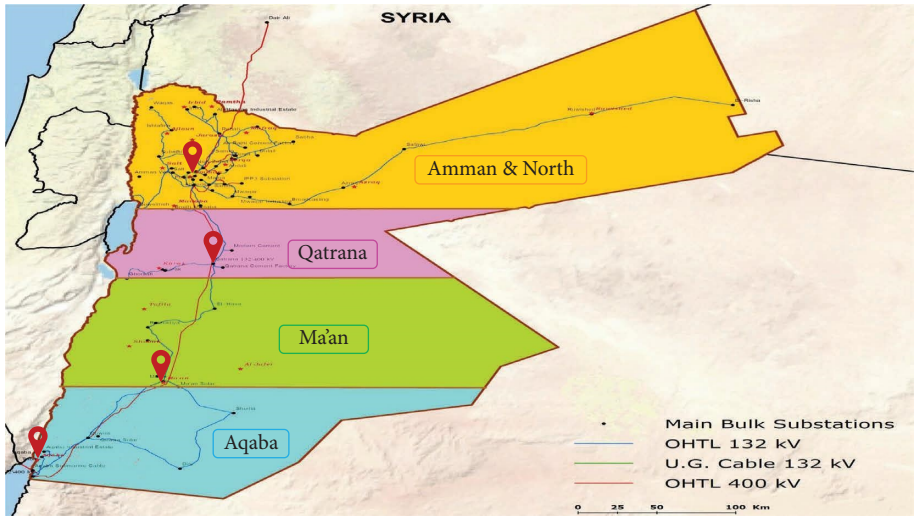

Figure 4: Aggregated systems map.

Table 1: Aggregated systems generation.

Aggregated system	Total nonrenewable (MW)	Total wind (MW)	Total PV (MW)
Aqaba	656	0	10
Ma'an	0	368	173.5
Qatrana	373	0	0
Amman and North	3316	1.57	232

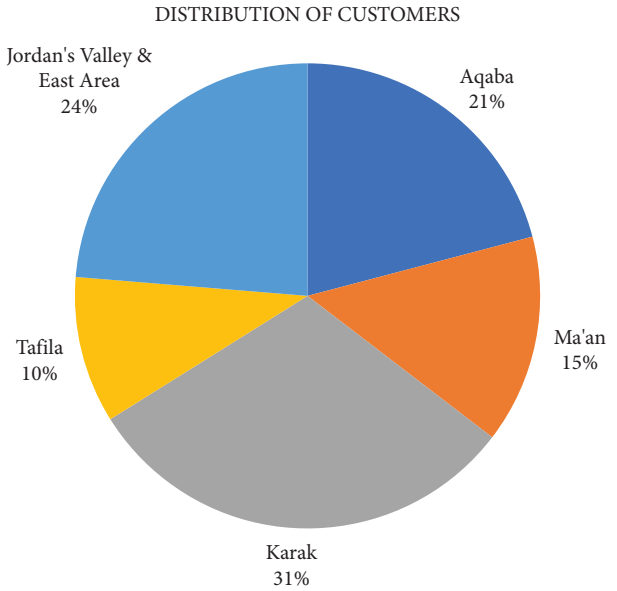

Figure 5: Customer distribution in EDCO regions.

The converter stations are thyristor-based and the DC voltage depends on the firing angle (α). Therefore, the value of the DC voltage is found using equation (8), where the nominal firing angle of the model is 15 degrees.

Table 2: Energy consumption for EDCO regions.

Region	Total consumption (GWh per year)
Aqaba	866.537
Jordan's Valley	1348.576
Suweimeh	477.336
Other southern cities	987.851
Total	3680.3

Table 3: Aggregated system's loads.

Aggregated system	Load (MW)
Aqaba	99
Ma'an	56
Qatrana	111
Amman and North	1829

$$U_{d\alpha} = U_{d0} \times \cos(\alpha), \tag{8}$$

$$U_{d\alpha} = 540.19 \cdot \cos(15^{\circ}) = 521.78\,kV. \tag{9}$$

The controlled characteristic used for the rectifier station is PDC control. The power setpoint for the converter station is set as 406 MW to maintain a consistent power flow as in the HVAC system. The design assures equivalent ratings to

Table 4: Transmission lines data of Jordan.

Voltage (kV)	R_L (Ω/km)	X_L (Ω/km)	R_0 (Ω/km)	X_0 (Ω/km)	S_{max} (MVA)	I_{rated} (kA)
132	0.0696	0.3913	0.3096	1.2644	160	0.7
400	0.0244	0.3094	0.9542	0.9542	600	0.866

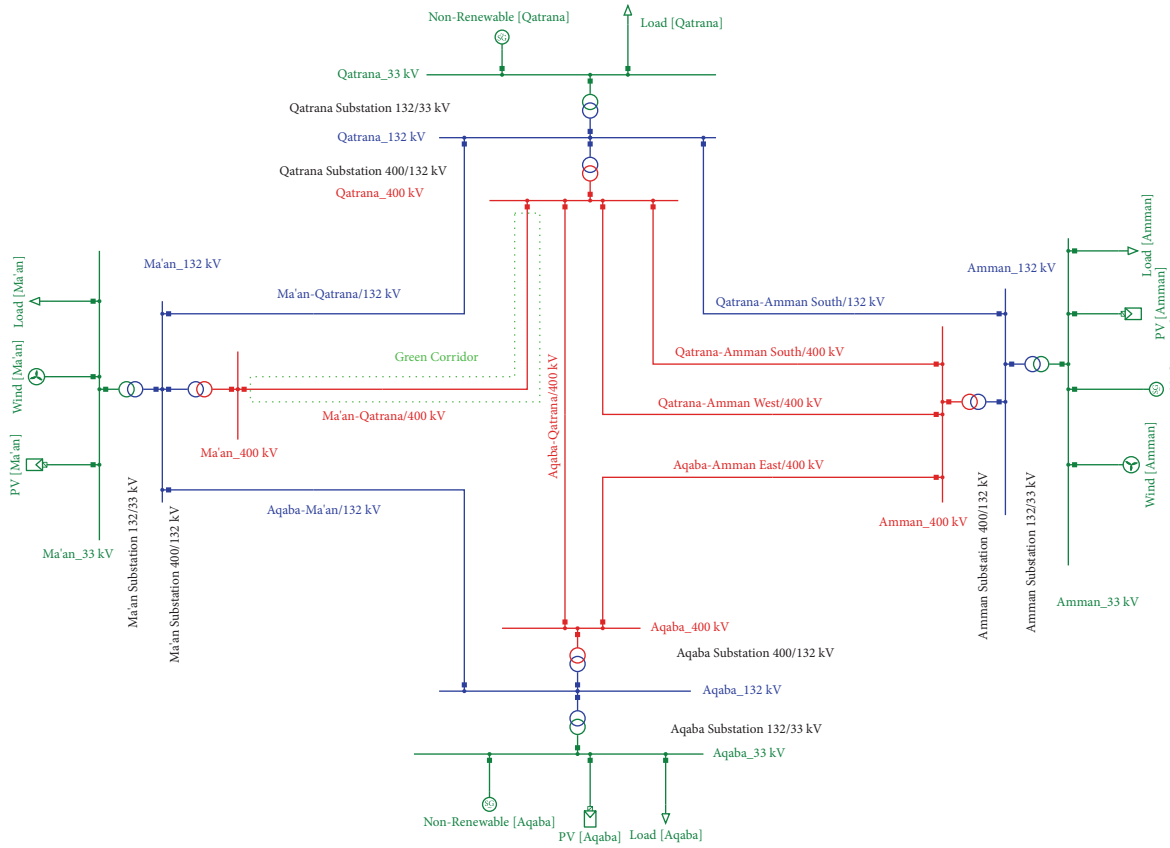

Figure 6: Jordan's model SLD.

maintain a fair comparison. Since the bipolar configuration is used, the positive link will transmit half of the power and the negative link will transmit the other half. The inverter station control characteristic is VDC, whereas the voltage setpoint is 1 p.u.

The commutation reactance for the converter station is 13.445 Ω based on the software-defined template. The tap-changer for the transformer is used as a fixed tap with a 30-degrees phase shift between the converters X and Y in each substation. The phase shift is established by using Yy-12 and Yd-11 transformers to reduce the low-order harmonics, especially the fifth and seventh harmonics [56–58].

4.3. Jordan's Model Using the VSC-HVDC Transmission System. The Green Corridor is designed as a VSC-HVDC transmission system, as shown in Figure 8. One of the main advantages of the VSC-HVDC over the LCC-HVDC transmission system is its ability to reverse the power flow. Consequently, pulse-width modulation (PWM) converters are installed at the terminals of the Green Corridor, where the power can flow in both directions. The installed PWM converter is a full-bridge modular multilevel converter (MMC) with an arm resistance of 6 mΩ and an inductance of 60 mH; these values are chosen based on the software-defined template.

VSC-HVDC systems are more flexible than LCC-HVDC; hence, more control options exist. However, controlling the reactive power at both ends is preferred to ensure minimum losses due to the lower currents. The power flow direction is set from Ma'an to Qatrana to maintain the same power flow for all system models. The DC voltage is 522 kV to maintain a fair comparison with the other systems. The inverter control mode is VDC-Q, where the DC voltage setpoint is 1 p.u., and the reactive power is zero MVAR.

5. Simulation Results and Discussion

Jordan's system is examined under different conditions using different power analysis functions to evaluate each system's performance under these conditions. Therefore, the HVDC systems' findings and contributions for enhancing the

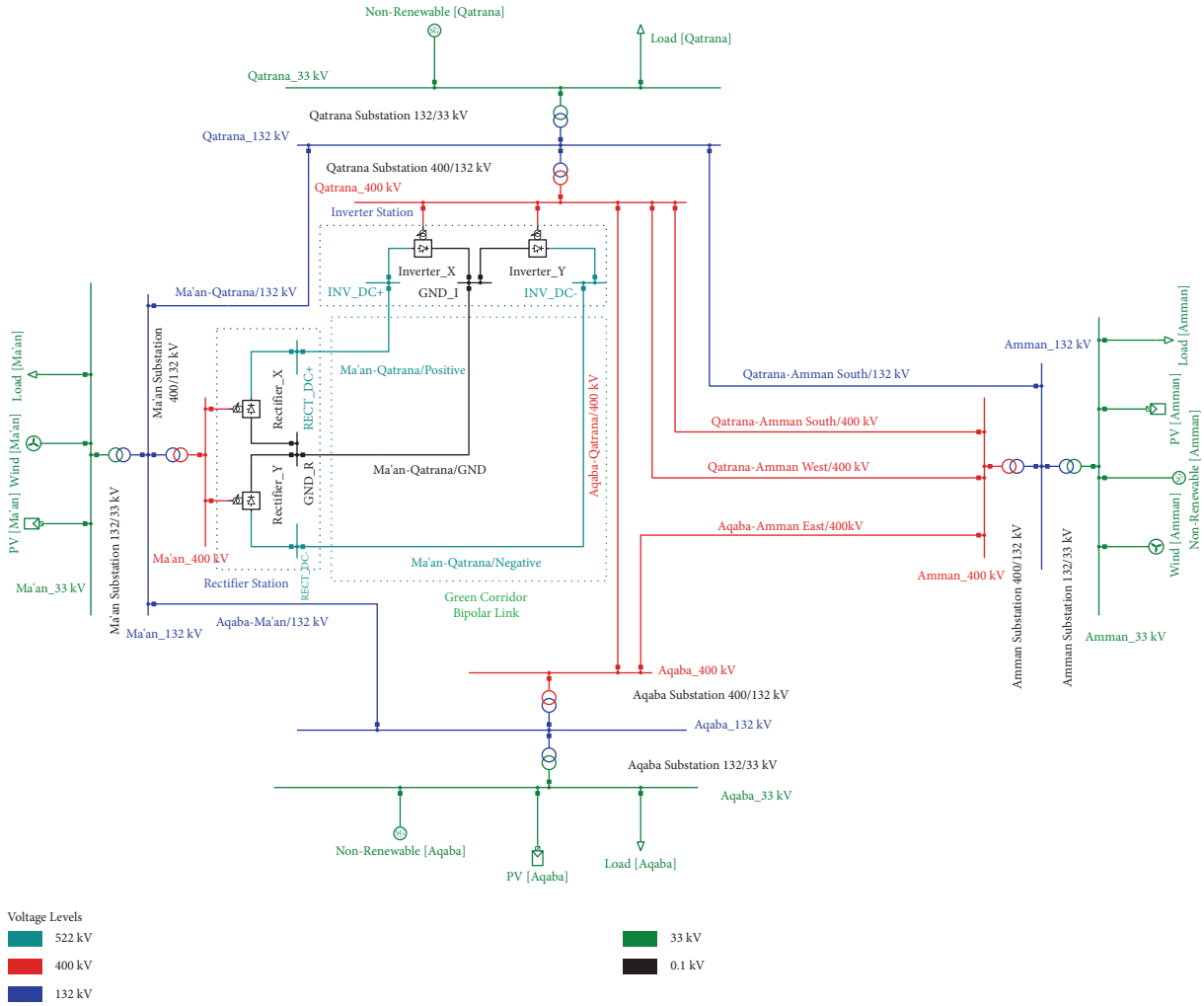

Figure 7: Jordan's model LCC-HVDC transmission system.

performance of Jordan's national grid are shown and compared with the HVAC transmission system using five scenarios, as shown in the following subsections. The converter stations' settings are maintained in all scenarios. In all simulations, the data are gathered from the software and tabulated for comparison, as there is no graphical way to show the results from the three different simulations together, and different analyses have different result visualization.

5.1. Scenario 1: Load Flow Analysis for Normal Conditions. In order to analyze the steady-state behavior of Jordan's network, a load flow analysis is conducted under normal operating conditions. The base scenario is established by considering the complete dispatch of renewable energy generation, representing the average load demand. This entails operating the PV and wind generation systems at their maximum capacities, reflecting their full potential contribution. Conventional power plants will contribute to balancing the active power of the system.

The variations in power flow and system performance between the different systems were observed. In addition, the power losses and transmission lines' capacities are compared for the different systems.

The differences between the three transmission systems are summarized in Table 5. The findings show that the HVDC systems outperformed the HVAC system. The HVDC Green Corridor has reduced the power losses by 70% compared to the HVAC transmission. Furthermore, the VSC-HVDC Green Corridor has lower power losses than the LCC-HVDC since the PWM converters do not consume reactive power, which leads to lower transmission current and lower power losses. However, it is worth mentioning that the LCC-HVDC system requires 129.9 MVAR of reactive power by the converter, which is about 35.19% of the active power by the converter, which may have a slight effect on the overall system power factor.

5.2. Scenario 2: Load Flow Analysis with PV System's Outage at "Amman and North". Due to the significance of the PV system in "Amman and North," the system is investigated when the aggregated system's PV generation experiences an outage, while the other renewable energy generations are fully dispatched. The losses between the different transmission systems are compared, in addition to examining the transmission line's capacity. The simulation results of the three transmission techniques are summarized in Table 6. It

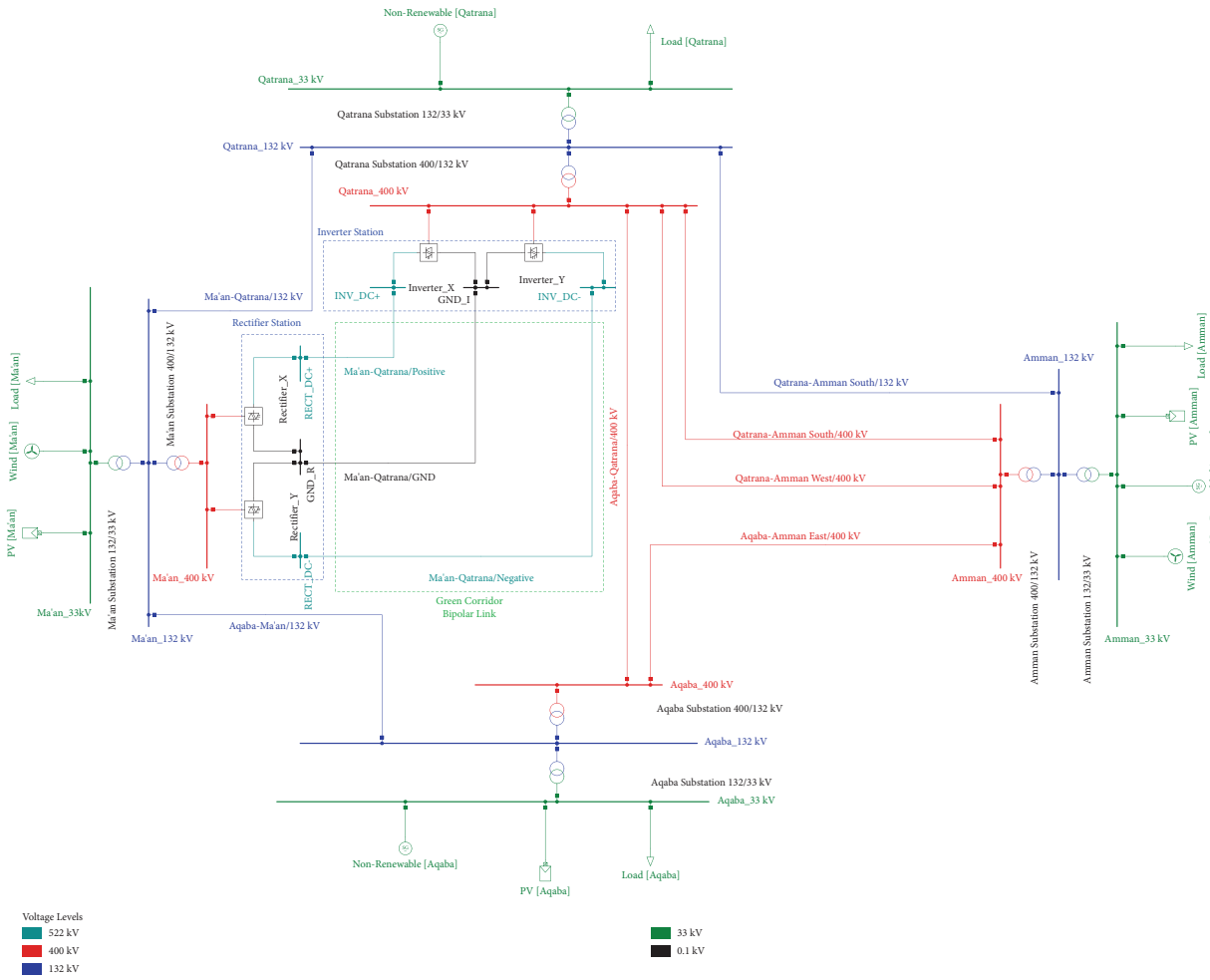

Figure 8: Jordan's model VSC-HVDC transmission system.

Table 5: Scenario 1 simulation result.

Metric	HVAC	LCC-HVDC	VSC-HVDC
Grid losses (MW)	4.02	2.78	2.69
Green Corridor losses (MW)	1.89	0.58	0.55
Green Corridor loading (%)	33.84	22.99	22.4

Table 6: Scenario 2 simulation results.

Metric	HVAC	LCC-HVDC	VSC-HVDC
Grid losses (MW)	4.27	3.08	2.99
Green corridor losses (MW)	1.92	0.58	0.55
Green corridor loading (%)	34.1	22.99	22.42

can be noticed that both HVDC systems have lower losses than the HVAC system. However, the losses in LCC-HVDC transmission are slightly higher than VSC-HVDC due to the higher current in the LCC-HVDC system. Again, in this scenario, the LCC-HVDC system requires 129.9 MVAR of reactive power by the converter, as the outage is not directly connected to the system's terminals and this mimics the conditions of the previous scenario.

5.3. Scenario 3: Three-Phase Short-Circuit at Ma'an's 400 kv Busbar. This scenario evaluates the different transmission systems subjected to a bolted three-phase short-circuit using the complete method at the sending terminal of the Green Corridor (Ma'an's 400 kV busbar), when the RES in the system are fully available. The short-circuit analysis will examine the short-circuit currents and power and the voltages at the busbars will be observed to compare the voltage changes between the different transmission systems.

As Ma'an's 400 kV busbar is only connected to the Green Corridor, the fault is appropriately isolated using the HVDC transmission systems. Comparisons between the HVDC and HVAC systems are shown in Table 7. The initial short-circuit power (S_{kss}), initial short-circuit current (I_{kss}), and peak short-circuit current (i_p) values at the fault location are significantly lower, proving HVDC systems' immunity against the fault. Moreover, the voltage variations at the busbars are considerably lower, demonstrating the higher voltage stability of HVDC transmission systems. For example, the "Amman and North" aggregated system voltage variations are 2.7%–3.4% when using the HVDC systems and are 17%–36.1% in HVAC systems.

Table 7: Scenario 3 simulation results.

Comparison		HVAC	LCC-HVDC	Difference* (%)	VSC-HVDC	Difference** (%)
Fault location	S_{kss} (MVA)	5249	1001.2	−80.93	1107.96	−78.89
	I_{kss} (kA)	7.577	1.445	−80.93	1.599	−78.90
	i_p (kA)	19.42	3.333	−82.84	3.688	−81.02
Aqaba	$\%\Delta V_{33kV}$	−21.26	−8.16	−61.62	−8.25	−61.19
	$\%\Delta V_{132kV}$	−23.68	−9.09	−61.61	−9.18	−61.23
	$\%\Delta V_{400kV}$	−24.69	−8.37	−66.10	−8.42	−65.90
Ma'an	$\%\Delta V_{33kV}$	−97.04	−96.19	−0.88	−96.22	−0.85
	$\%\Delta V_{132kV}$	−97.04	−96.19	−0.88	−96.22	−0.85
	$\%\Delta V_{400kV}$	−100	−100	0.00	−100	0.00
Qatrana	$\%\Delta V_{33kV}$	−30.04	−6.11	−79.66	−6.1	−79.69
	$\%\Delta V_{132kV}$	−33.55	−6.83	−79.64	−6.83	−79.64
	$\%\Delta V_{400kV}$	−36.14	−5.38	−85.11	−5.39	−85.09
Amman and North	$\%\Delta V_{33kV}$	−16.99	−2.81	−83.46	−2.76	−83.76
	$\%\Delta V_{132kV}$	−18.86	−3.12	−83.46	−3.11	−83.51
	$\%\Delta V_{400kV}$	−20.66	−3.41	−83.49	−3.44	−83.35

*Difference of LCC-HVDC with respect to HVAC. **Difference of VSC-HVDC with respect to HVAC.

5.4. Scenario 4: Contingency Analysis for the Green Corridor. The robustness and reliability of the system are assessed in this scenario by applying the N-1 contingency analysis to the Green Corridor double-circuit transmission line, i.e., the Green Corridor works as a single circuit only when the other line is disconnected during the contingency. The differences in the power flow, power losses, and transmission capacity of the system are observed for the three transmission systems. Any violations are also reported.

When using HVAC, the loading on the Green Corridor increases from 33.8% to 59.4% due to the N-1 contingency event. The Green Corridor transmits 356 MW during contingency compared to 406 MW under normal conditions. The balance is distributed on the other lines, which changes the system's power flow, leading to an increase in the system's losses. The overall system losses increased by 63.21% (from 4.02 to 6.56 MW) and the Green Corridor losses increased by 53.44% (from 1.89 to 2.9 MW).

When using the LCC-HVDC Green Corridor, the power flow changes in the system are negligible. The LCC-HVDC Green Corridor maintained the power flow with the same amount of transmitted power due to its capability to handle more power capacity during contingency. All loadings and voltages are kept at the same value, except the losses in the Green Corridor which increased by 172% (from 0.58 to 1.58 MW) due to transmitting more power. However, the overall losses have increased by only 20.7% (from 2.78 MW to 3.35 MW).

When using VSC-HVDC, the results demonstrate that the system handles the contingency appropriately, since it maintained the same power flow during the contingency event. The Green Corridor still transmits the same amount of power while the rest of the system is not affected. The loading of the Green Corridor is doubled. Therefore, the losses increased by 100% (from 0.55 MW to 1.1 MW) and the overall system losses increased by 20.34% (from 2.69 MW to 3.24 MW).

The N-1 contingency event is handled correctly when using the HVDC transmission systems without changing the power flow in the system. Consequently, the increase in the overall losses in the system is much lower than that of the HVAC transmission system. This scenario demonstrated the capability of transmitting more power in HVDC lines. A sample of the simulation results is shown in Figure 9. It is worth mentioning that HVDC systems are more resilient to partial line outages, for example, if one of the polarities experiences an outage, partial proportionate operation is still possible. However, this is only possible under open delta conditions in AC systems, which is not typical in transmission.

5.5. Scenario 5: Stability Analysis for Qatrana's Synchronous Generator during a Busbar Three-Phase Fault. The RMS simulation tool is used in this scenario for stability analysis and to evaluate the system's dynamics. The event is a three-phase short-circuit with a duration of 0.08 seconds applied on the transmission line terminal at Qatrana's 33 kV busbar. It should be noted that all protection devices are considered inactive during this analysis; in other words, all relays and circuit breakers are disabled.

The "Amman and North" conventional generator is the reference machine, as it is the largest nonrenewable generation in the network. The conventional generation at Qatrana is represented by a synchronous generator and is examined to determine its active power and the rotor's speed and angle. In addition, the CCT will be determined.

Using HVAC, the active power, rotor speed, and rotor angle of the synchronous generator at Qatrana are shown in Figure 10. The fault is cleared in 0.58 seconds. At this time, the active power rises to its maximum value of 626.2 MW and then starts to oscillate, reaching a steady-state in 9.5 seconds, as shown in Figure 11. The rotor speed starts to increase during the fault until the fault is cleared. During the

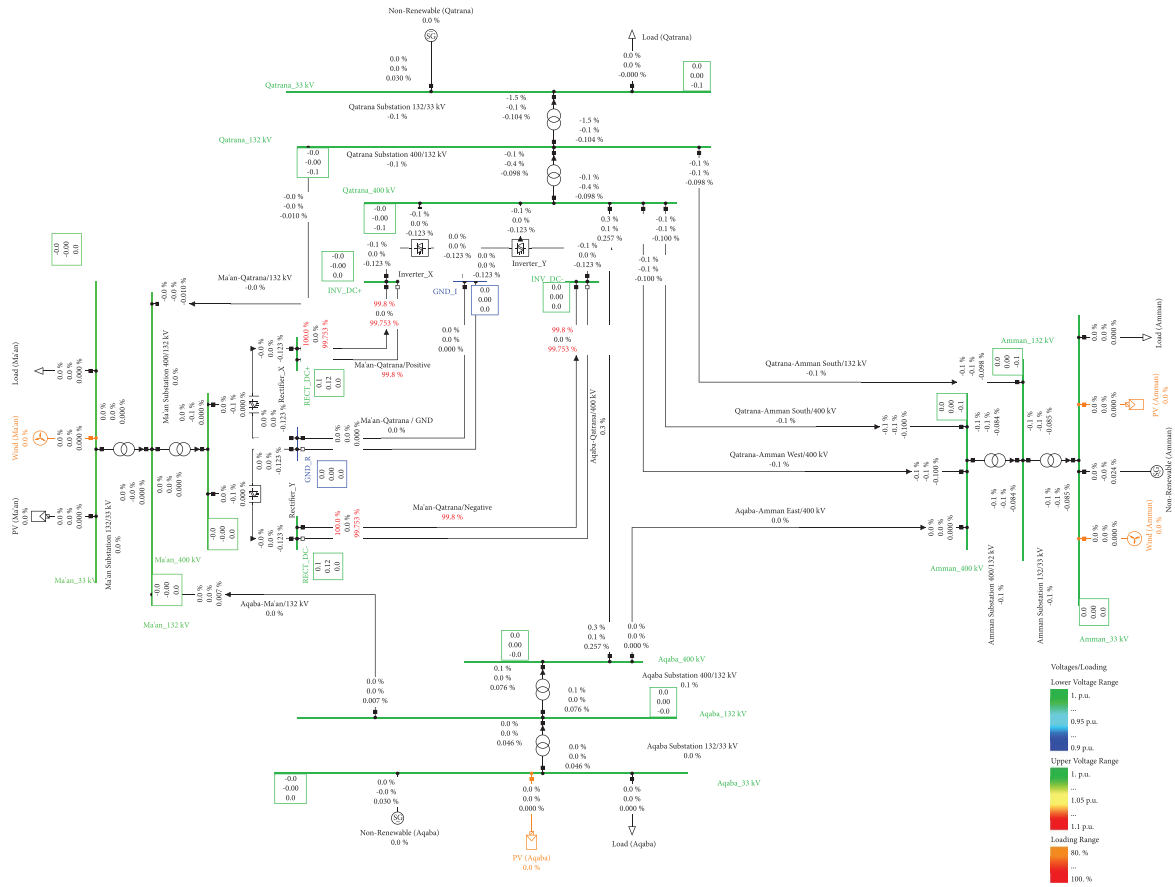

Figure 9: Contingency analysis for VSC-HVDC Green Corridor.

recovery process, the rotor angle still has kinetic energy from the fault event and reaches a maximum value of 1.008 p.u. and settles down in 74.8 seconds. The synchronous generator behavior is illustrated in the power angle curve, shown in Figure 12.

At the beginning of the event, the active power falls to zero immediately, where the rotor angle remains at the initial value due to the rotor's inertia. As the rotor speeds up, the rotor angle increases until the fault is cleared. At this point, the power rises with an oscillating behavior, and the rotor speed starts to decelerate, maintaining a stable condition. The rotor angle oscillates between 68.33 and 162.05 degrees until it is 51.28 degrees, which is the same as the initial condition. Therefore, the synchronous generator stays in synchronism during this event and the CCT is 296 ms.

By using LCC-HVDC, the active power reaches a maximum value of 662.8 MW and then starts to oscillate. However, the LCC-HVDC converters experienced a commutation failure during the postfault recovery process, resulting in instability on the AC side, as illustrated in Figure 13. Losing synchronism leads to a continuous increase in the rotor speed, where the rotor angle swings between −180 and 180 degrees, known as a pole-slip. The active power fluctuates between −201.2 MW and 262.9 MW. The power angle curve is illustrated in Figure 14.

When using VSC-HVDC, the active power reaches a maximum value of 718.9 MW during the postfault recovery process and starts to oscillate, settling at 373 MW in 6 seconds. Both rotor speed and rotor angle oscillate until they reach the steady state in 6.1 seconds, maintaining stable conditions. The active power, rotor speed, and rotor angle of the synchronous generator at Qatrana are shown in Figures 15 and 16. The power angle curve, shown in Figure 17, illustrates the rotor angle swinging between 63.4 and 38.9 degrees during the deceleration process, reaching steady-state, which is the same as the initial condition. The synchronous generator remains in synchronism and the CCT is 303 ms.

This analysis showed the differences between HVAC, LCC-HVDC, and VSC-HVDC systems in terms of stability. The results validate that VSC-HVDC has the best performance since the system reached the steady-state conditions in a shorter time and has longer CCT compared to the other techniques. In contrast, the LCC-HVDC system suffers from commutation failure during the recovery process affecting the grid's stability. This issue can be solved by employing auxiliary synchronous condensers but this solution adds complexity and cost. In the HVAC case, the rotor angle swinging range is extensive and has lower CCT.

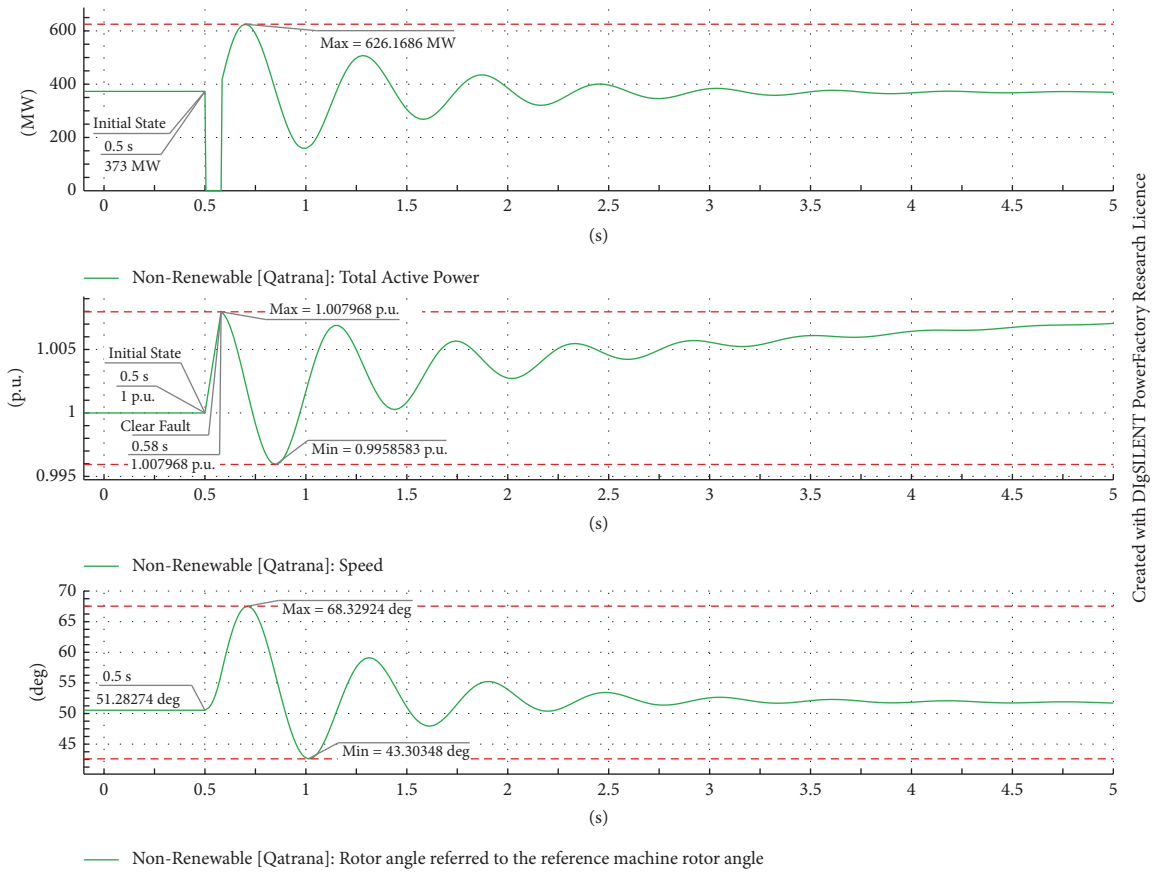

Figure 10: 5-second RMS simulation for Qatrana-HVAC Green Corridor.

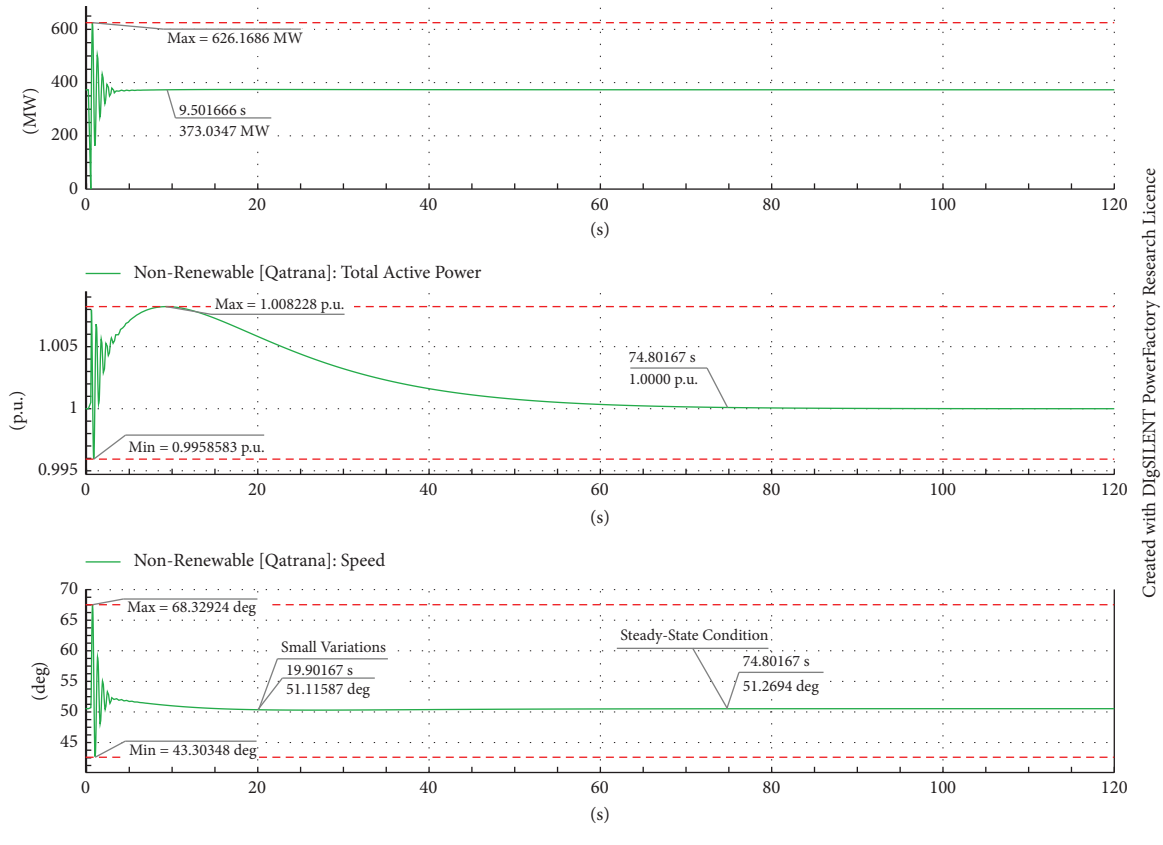

Figure 11: 120-second RMS simulation for Qatrana-HVAC Green Corridor.

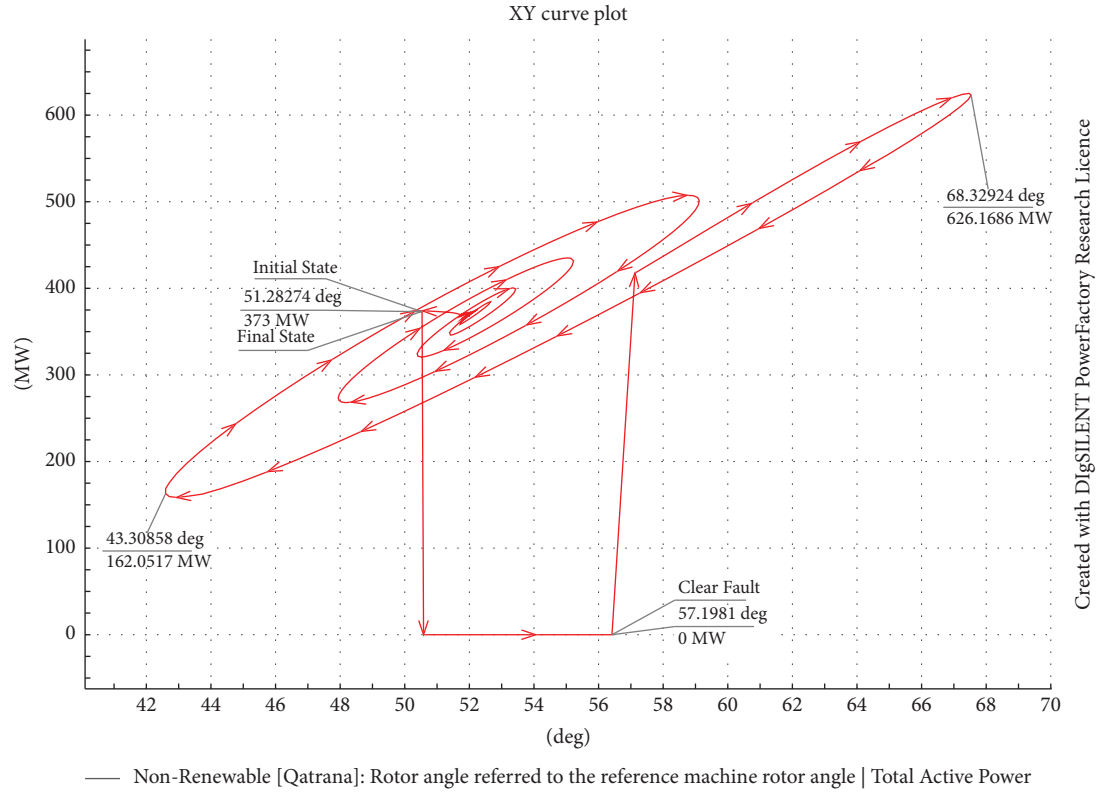

Figure 12: Power angle curve for Qatrana-HVAC Green Corridor.

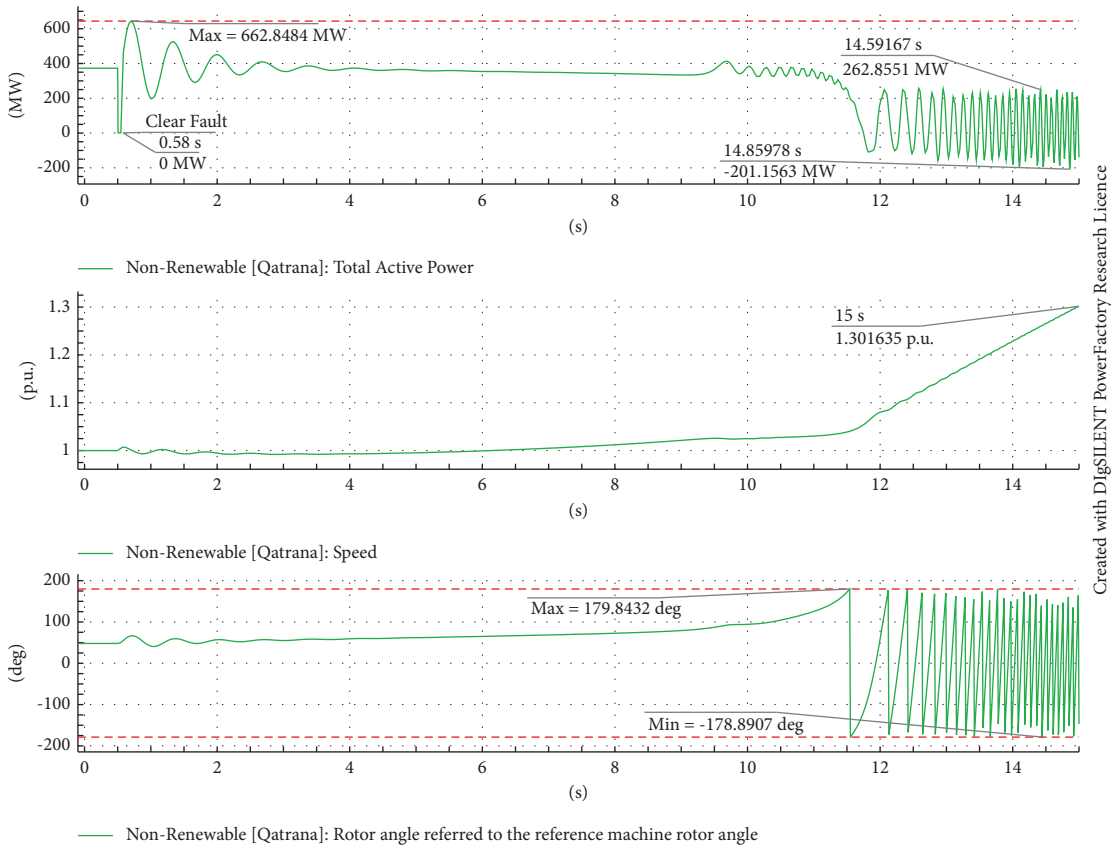

Figure 13: LCC-HVDC Green Corridor commutation failure.

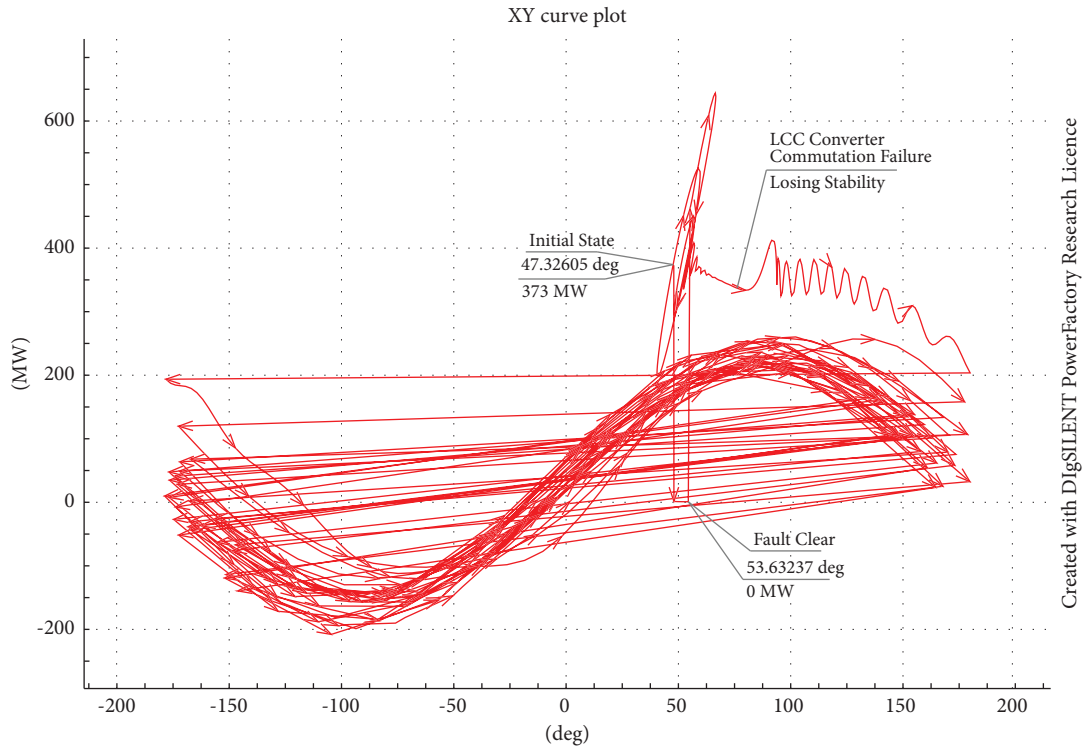

Figure 14: Power angle curve for Qatrana-LCC-HVDC Green Corridor (commutation failure).

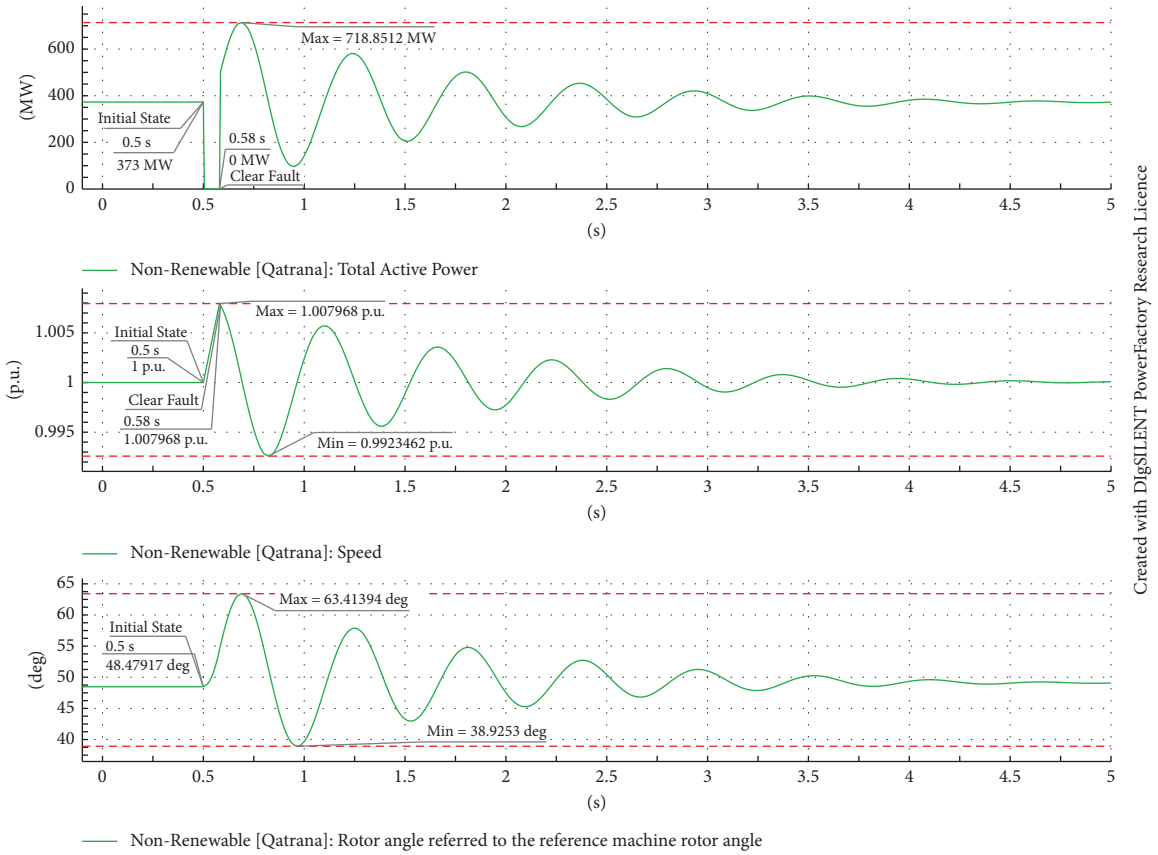

Figure 15: 5-second RMS simulation for Qatrana-VSC-HVDC Green Corridor.

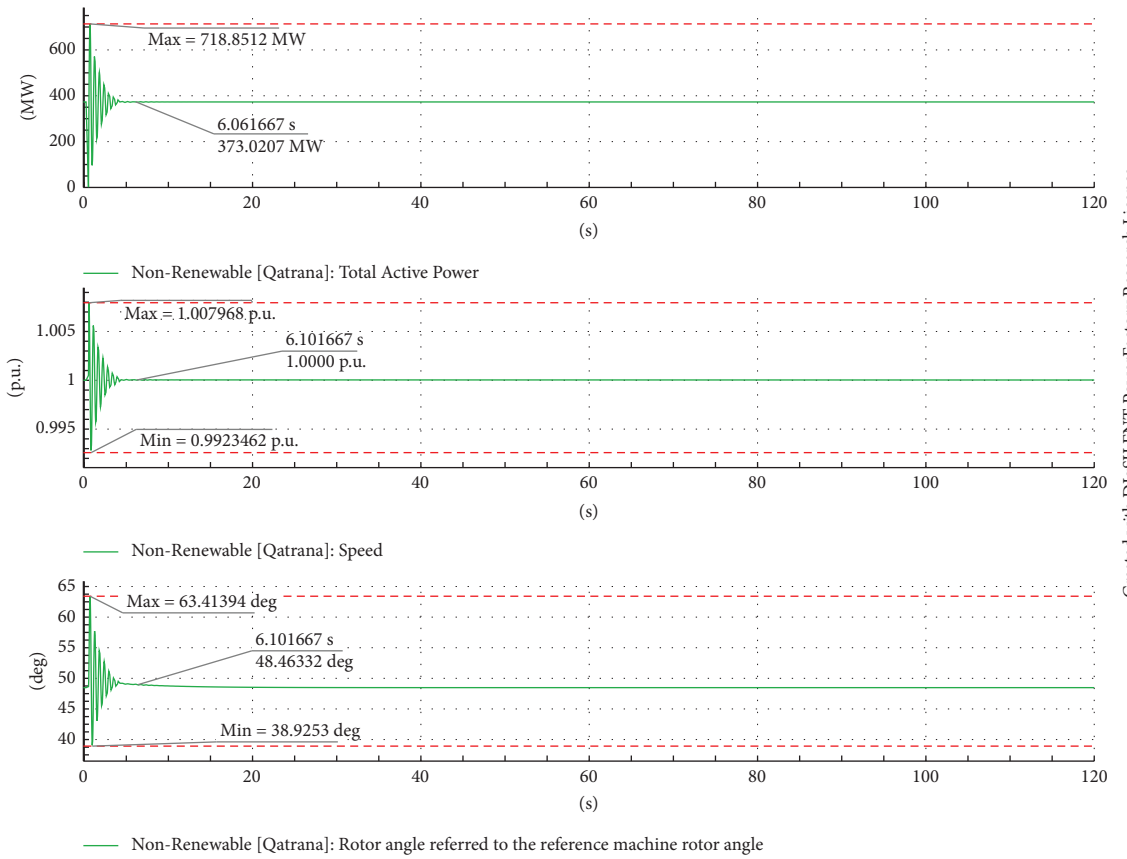

Figure 16: 20-second RMS simulation for Qatrana-VSC-HVDC Green Corridor.

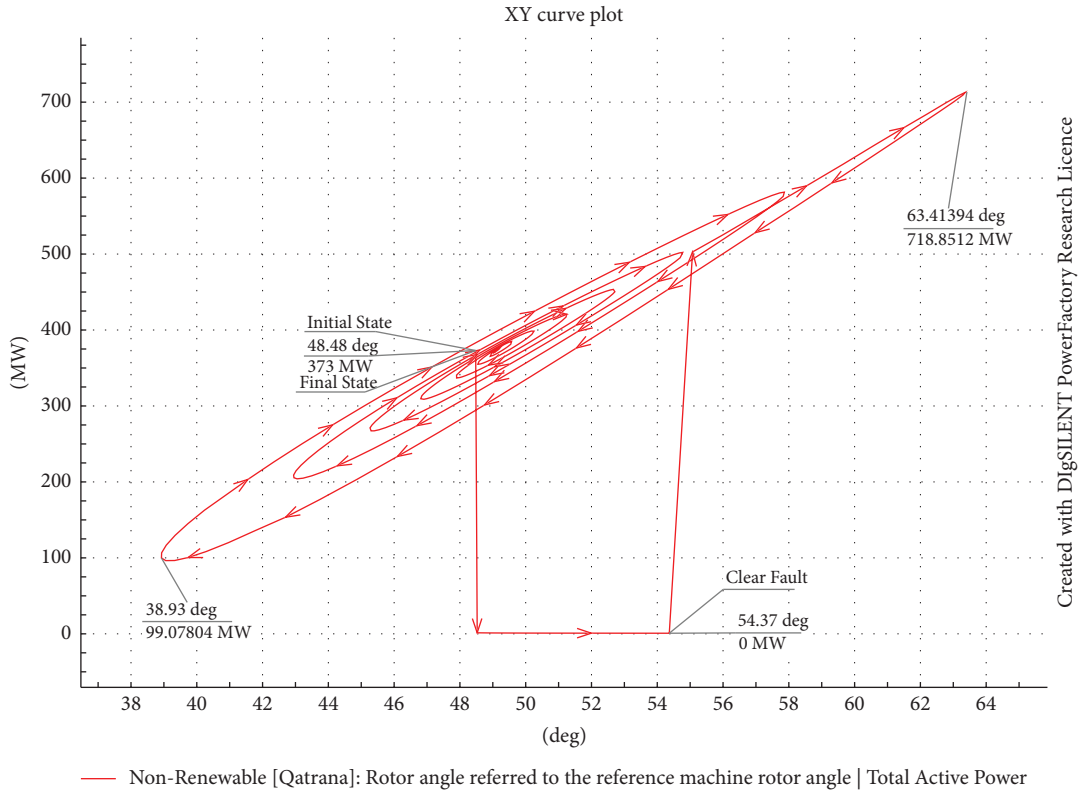

Figure 17: Power angle curve for Qatrana-VSC-HVDC Green Corridor.

5.6. Overall Discussion. As can be seen in the above-mentioned results, the HVDC transmission systems outperformed HVAC by proving their merits in several scenarios, such as having lower losses and higher transmission capacity. Moreover, HVDC systems are immune to fault conditions since they perform as barriers, keeping lower voltage variations and lower short-circuit currents. HVDC systems can handle contingency events suitably since they maintain the same power flow and have the feature of higher capacity.

However, it is notable that LCC-HVDC converters require more reactive power and are susceptible to commutation failure. Using commutation failure elimination equipment such as TBCC increases the cost and complexity of the system. As a result, the VSC-HVDC system is the best option for transmitting the RES energy from the southern part of the country to the central area by considering the different aspects.

6. Conclusion

This study examined the different transmission approaches that can be integrated into an existing HVAC power system with a high penetration of renewable energy resources. Two types of HVDC systems are proposed: LCC-HVDC and VSC-HVDC.

The Green Corridor in Jordan's national electric grid was chosen as a case study. All generation, transmission, and distribution characteristics are modeled during the study to conduct a realistic system investigation. The HVDC transmission system is integrated into a comprehensive system to examine and observe the grid's overall performance, reaction, and recovery process.

The results show that both the HVDC transmission systems outperform the HVAC due to their lower transmitted power losses and higher capacity features. The transmitted power losses are reduced by 70% when using the HVDC systems. This negates any additional HVAC line installation, avoiding violating the ROW. The VSC-HVDC system often does not consume reactive power and has better voltage magnitudes, which leads to lower power losses than the LCC-HVDC system.

HVDC systems handled contingency events better than HVAC due to their high reliability and high transmission capacity, which leads to sustaining high power transmission during a contingency event without stressing the transmission line loading. Furthermore, the investigations during short-circuit events proved that the voltage stability of the HVDC is remarkably better than that of the HVAC system by appearing as a barrier against faults.

The stability analysis showed that the CCT is longer when integrating HVDC systems than when integrating HVAC. Nonetheless, it is worth noting that LCC-HVDC systems may suffer a commutation failure issue during the post-fault recovery process due to the physical properties of the thyristors, which affects the stability of the AC side. On the other hand, VSC-HVDC systems have increased the grid's stability by settling the rotor angle and rotor speed faster than the other systems. Also, VSC-HVDC systems do not demonstrate any problems during the post-fault recovery process.

In conclusion, the VSC-HVDC benefits outweigh both HVAC and LCC-HVDC in terms of power losses, capacity, and stability. Moreover, VSC-HVDC systems are more flexible due to more control options, e.g., the active and reactive powers can be controlled independently. Whereas, in LCC-HVDC systems, the reactive power is a function of the active power; hence, it cannot be controlled. Finally, the overall results confirm that the VSC-HVDC approach serves as a better alternative than both HVAC and LCC-HVDC systems, as it was demonstrated in the Green Corridor transmission line case study.

As this topic is vast and there are several avenues for expansion, future work may include the effect of generation scheduling and power flow, integrating system protection and relay settings, requirements for DC circuit breakers, optimization to minimize the HVDC transmission systems integration cost, AC and DC harmonic filters, and grid connection with other systems.

Data Availability

The data used to support the findings of this study are included within the article.

Disclosure

DIgSILENT LLC provided the PowerFactory4'esis license (PF4T) which was used in this study.

Conflicts of Interest

The authors declare that they have no conflicts of interest regarding the publication of this paper.

Acknowledgments

This work was financially supported by the deanship of scientific research at the German Jordanian University.

References

[1] A. Constantin and R. Dinculescu, "Impact in the power system following the replacement of HVAC with HVDC lines in Dobrogea area," in *Proceedings in the 2019 8th International Conference on Modern Power Systems (MPS)*, pp. 1–5, Cluj, Romania, May 2019.

[2] G. Ren, J. Liu, J. Wan, Y. Guo, and D. Yu, "Overview of wind power intermittency: impacts, measurements, and mitigation solutions," *Applied Energy*, vol. 204, pp. 47–65, Oct. 2017.

[3] A. Clerici, L. Paris, and P. Danfors, "HVDC conversion of HVAC lines to provide substantial power upgrading," *IEEE Transactions on Power Delivery*, vol. 6, no. 1, pp. 324–333, Jan. 1991.

[4] Z. M. Dalala, "Energy harvesting using thermoelectric generators," in *Proceedings in the 2016 IEEE International Energy*

Conference (ENERGYCON), pp. 1–6, Leuven, Belgium, April 2016.

[5] Z. Dalala, T. Alwahsh, and O. Saadeh, "Energy recovery control in elevators with automatic rescue application," *Journal of Energy Storage*, vol. 43, Article ID 103168, 2021.

[6] O. Saadeh, A. Al Nawasrah, and Z. Dalala, "A bidirectional electrical vehicle charger and grid interface for grid voltage dip mitigation," *Energies*, vol. 13, no. 15, p. 3784, 2020.

[7] L. Michi, "An overview of the HVDC transmission system models in planning tools: the Italian experience," in *Proceedings in the 2019 AEIT HVDC International Conference (AEIT HVDC)*, pp. 1–6, Florence, Italy, May 2019.

[8] A. Kalair, N. Abas, and N. Khan, "Comparative study of HVAC and HVDC transmission systems," *Renewable and Sustainable Energy Reviews*, vol. 59, pp. 1653–1675, 2016.

[9] N. F. Ibrahim and S. S. Dessouky, "Design and implementation of voltage source converters in HVDC systems," in *Power Systems*, Springer International Publishing, Berlin, Germany, 2021.

[10] M. P. Bahrman and B. K. Johnson, "The ABCs of HVDC transmission technologies," *IEEE Power and Energy Magazine*, vol. 5, no. 2, pp. 32–44, 2007.

[11] A. Alassi, S. Bañales, O. Ellabban, G. Adam, and C. MacIver, "HVDC transmission: technology review, market trends and future outlook," *Renewable and Sustainable Energy Reviews*, vol. 112, pp. 530–554, Sep. 2019.

[12] N. B. Negra, J. Todorovic, and T. Ackermann, "Loss evaluation of HVAC and HVDC transmission solutions for large offshore wind farms," *Electric Power Systems Research*, vol. 76, no. 11, pp. 916–927, Jul. 2006.

[13] C. Joe-Uzuegbu and G. Chukwudebe, "High Voltage Direct Current (HVDC) technology: an alternative means of power transmission," in *Proceedings of the 3rd IEEE International Conference on Adaptive Science and Technology (ICAST 2011)*, Abuja, Nigeria, November 2011.

[14] G. Arcia-Garibaldi, P. Cruz-Romero, and A. Gómez-Expósito, "Future power transmission: visions, technologies and challenges," *Renewable and Sustainable Energy Reviews*, vol. 94, pp. 285–301, Oct. 2018.

[15] M. P. Bahrman, "Overview of HVDC transmission," in *Proceedings of the 2006 IEEE PES Power Systems Conference and Exposition*, pp. 18–23, Chicago, IL, USA, October 2006.

[16] O. Saadeh, B. A. Sba, Z. Dalala, and A. Bashaireh, "Comparative performance analysis of HVDC and HVAC transmission systems in the presence of PV generation: a case study using the IEEE-5-bus network," in *Proceedings of the 2023 AEIT HVDC International Conference (AEIT HVDC)*, pp. 1–5, Rome, Italy, May 2023.

[17] M. H. Okba, M. H. Saied, M. Z. Mostafa, and T. M. A. Moneim, "High voltage direct current transmission-a review, part i," in *Proceedings of the 2012 IEEE Energytech*, pp. 1–7, Cleveland, OH, USA, May 2012.

[18] J. P. Novoa and M. A. Rios, "Conversion of HVAC lines into HVDC in transmission expansion planning," *International Journal of Energy and Power Engineering*, vol. 11, no. 12, p. 7, 2017.

[19] A. Beddard and M. Barnes, "Hvdc cable modelling for vsc-hvdc applications," in *Proceedings of the 2014 IEEE PES General Meeting Conference and Exposition*, pp. 1–5, National Harbor, MD, USA, July 2014.

[20] M. Moradi-Sepahvand and T. Amraee, "Hybrid AC/DC transmission expansion planning considering HVAC to HVDC conversion under renewable penetration," *IEEE Transactions on Power Systems*, vol. 36, no. 1, pp. 579–591, Jan. 2021.

[21] L. Colla, M. Rebolini, S. Malgarotti, and U. Zanetta, "Analysis on the possible conversion of overhead lines from AC to DC," *Papers and proceedings*, vol. 2, 2010.

[22] R. Benato, S. D. Sessa, G. Gardan, and A. L'Abbate, "Converting overhead lines from HVAC to HVDC: an overview analysis," in *Proceedings of the 2021 AEIT HVDC International Conference (AEIT HVDC)*, pp. 1–6, Genoa, Italy, May 2021.

[23] I. Tc/Sc 36, *iec/tr 60815 ed. 1.0 b:1986, Guide For the Selection of Insulators in Respect of Polluted Conditions*, Distributed through American National Standards Institute, Washington, DC, USA, 2007.

[24] D. M. Larruskain, I. Zamora, O. Abarrategui, and Z. Aginako, "Conversion of AC distribution lines into DC lines to upgrade transmission capacity," *Electric Power Systems Research*, vol. 81, no. 7, pp. 1341–1348, Jul. 2011.

[25] O. E. Oni, I. E. Davidson, and K. N. I. Mbangula, "A review of LCC-HVDC and VSC-HVDC technologies and applications," in *Proceedings of the 2016 IEEE 16th International Conference on Environment and Electrical Engineering (EEEIC)*, pp. 1–7, Florence, Italy, January 2016.

[26] M. P. González and M. A. Ríos, "Comparison of hvdc-grid and hvac into transmission expansion planning," in *Proceedings of the 2018 IEEE ANDESCON*, pp. 1–5, Santiago de Cali, Colombia, August 2018.

[27] S. Azzam, E. Feilat, and A. Al-Salaymeh, "Impact of connecting renewable energy plants on the capacity and voltage stability of the national grid of jordan," in *Proceedings of the 2017 8th International Renewable Energy Congress (IREC)*, pp. 1–6, Amman, Jordan, March 2017.

[28] M. Migliori, S. Lauria, L. Michi, G. Donnini, B. Aluisio, and C. Vergine, "Renewable sources integration using HVDC in parallel to AC traditional system: the Adriatic project," in *Proceedings of the 2019 AEIT HVDC International Conference (AEIT HVDC)*, pp. 1–5, Florence, Italy, May 2019.

[29] O. Stanojev, J. Garrison, S. Hedtke, C. M. Franck, and T. Demiray, "Benefit analysis of a hybrid hvac/hvdc transmission line: a swiss case study," in *Proceedings of the 2019 IEEE Milan PowerTech*, pp. 1–6, Milan, Italy, June 2019.

[30] M. Gul, N. Tai, W. Huang, M. H. Nadeem, M. Ahmad, and M. Yu, "Technical and economic assessment of VSC-HVDC transmission model: a case study of south-western region in Pakistan," *Electronics*, vol. 8, no. 11, p. 1305, 2019.

[31] M. M. Samy, "Computation of electromagnetic fields around HVDC transmission line tying Egypt and KSA," in *Proceedings of the 2017 Nineteenth International Middle East Power Systems Conference (MEPCON)*, pp. 1276–1280, Cairo, Egypt, December 2017.

[32] M. Samy, A. El-Zein, and M. Abdel-Salam, "Electric field profiles and right-of-way widths as influenced by grounded shield wires underneath EHV direct current transmission Lines," *The International Conference on Electrical Engineering*, vol. 6, no. 6, pp. 1–12, May 2008.

[33] A. Elmorshdy, M. M. Samy, and A. M. Emam, "Field profiles underneath and between proposed hybrid power lines in Egyptian grid," in *Proceedings of the 2019 21st International Middle East Power Systems Conference (MEPCON)*, pp. 724–730, Cairo, Egypt, December 2017.

[34] A. T. Mohamed, A. Elmorshdy, A. M. Emam, and M. M. Samy, "Optimum configuration for higher transmission ratings for proposed hybrid overhead power lines in Egypt electric utility," in *Proceedings of the 2021 22nd*

International Middle East Power Systems Conference (MEPCON), pp. 665–671, Assiut, Egypt, December 2021.

[35] cigre, ""Influence of embedded HVDC transmission on system security and AC network performance," e-cigre," 2020, https://e-cigre.org/publication/536-influence-of-embedded-hvdc-transmission-on-system-security-and-ac-network-performance.

[36] IEEE, "IEEE recommended practice for the design of dc auxiliary power systems for generating stations," *IEEE Std*, vol. 52, pp. 1–35, 1993.

[37] I. Tc/Sc 73, *IEC 61660-1 ed. 1.0 b:1997, Short-Circuit Currents in d.c. Auxiliary Installations in Power Plants and Substations-Part 1: Calculation of Short-Circuit Currents*, Distributed through American National Standards Institute, Washington, DC, USA, 2007.

[38] I. Tc/Sc 18, *IEC 61363-1 Ed. 1.0 B:1998, Electrical Installations of Ships and mobile and Fixed Offshore Units- Part 1: Procedures For Calculating Short-Circuit Currents in Three-phase a.C. Multiple*, Distributed through American National Standards Institute, Washington, DC, USA, 2007.

[39] IEEE, "IEEE guide for calculation of fault currents for application of AC high-voltage circuit breakers rated on a total current basis," *ANSI IEEE*, vol. 375, pp. 1–24, 1979.

[40] digsilent, "Powerfactory 2021 user manual," 2020, https://www.digsilent.de.

[41] D. Sweeting, "Applying IEC 60909, short-circuit current calculations," in *Proceedings of the 2011 Record of Conference Papers Industry Applications Society 58th Annual IEEE Petroleum and Chemical Industry Conference (PCIC)*, pp. 1–6, Toronto, Canada, September 2011.

[42] J. D. Glover, M. S. Sarma, and T. J. Overbye, "Power system analysis and design," *Global Engineering*, Cengage Learning, Boston, MA, USA, 5th edition, 2010.

[43] V. J. Mishra and M. D. Khardenvis, "Contingency analysis of power system," in *Proceedings of the 2012 IEEE Students' Conference on Electrical, Electronics and Computer Science*, pp. 1–4, Bhopal, India, March 2012.

[44] R. Bacher, "Graphical interaction and visualization for the analysis and interpretation of contingency analysis results," in *Proceedings of Power Industry Computer Applications Conference*, pp. 128–134, Salt Lake City, UT, USA, May 1995.

[45] IEEE, "IEEE Recommended Practice for Conducting Short-Circuit Studies and Analysis of Industrial and Commercial Power Systems," *IEEE Std*, vol. 23, pp. 1–184, 2019.

[46] C. R. Bayliss and B. J. Hardy, "Chapter 23- distribution planning," in *Transmission and Distribution Electrical Engineering*, C. R. Bayliss and B. J. Hardy, Eds., Newnes, Oxford, UK, 4th edition, 2012.

[47] T. Gonen, *Electric Power Distribution Engineering*, CRC Press, Boca Raton, FL, USA, 3rd edition, 2015.

[48] EDCO, *EDCO Annual Report 2020*, Electricity Distribution Company, Amman, Jordan, 2020.

[49] IDECO, *IDECO Annual Report 2019*, https://www.ideco.com.jo/portal/OtherFiles/AnnualReport2019.pdf, Irbid District Electricity Company Ltd, Amman, Jordan, 2019, https://www.ideco.com.jo/portal/OtherFiles/AnnualReport2019.pdf.

[50] CEGCO, *CEGCO Annual Report 2019*, Central Electricity Generation Co, Amman, Jordan, 2019, https://www.cegco.com.jo/Admin_Site/Files/PDF/d743b242-9727-4108-909a-3a2e68a5a8a3.pdf.

[51] NEPCO, *NEPCO Annual Report 2019*, National Electric Power Company, Amman, Jordan, 2019, https://www.nepco.com.jo/store/DOCS/web/2019_en.pdf.

[52] M. Schmieg, "DIgSILENT PowerFactory," 2022, https://www.digsilent.de/en/.

[53] D. T. Oyedokun and K. A. Folly, "Network transient responses to varying HVAC line length along a HVDC transmission corridor," *IEEE Africon '11*, vol. 11, pp. 1–6, 2011.

[54] A. S. Al-akayshee, O. N. Kuznetsov, and H. M. Sultan, "Modelling and performance evaluation of the 400kV national grid in Iraq in DigSILENT PowerFactory," in *Proceedings of the 2020 IEEE Conference of Russian Young Researchers in Electrical and Electronic Engineering (EIConRus)*, pp. 1151–1156, Moscow, Russia, January 2020.

[55] R. Faizal, M. Nurdin, N. Hariyanto, S. Pack, and J. Plesch, "Sumatra-java hvdc transmission system modelling and system impact analysis," in *Proceedings of the 2015 IEEE Eindhoven PowerTech*, pp. 1–6, Eindhoven, Netherlands, June 2015.

[56] B. Jucker and M. Heimbach, "Special Report on Transformers,," *ABB's Corporate Technical Journal*, 2012, https://library.e.abb.com/public/c3791bac5b25bd10c1257ab80037553b/ABB%20SR%20Transformers-121031.pdf.

[57] Z. Du, Y. Yang, J. Yang, J. Chen, T. Sun, and H. Mao, "Study on DC side harmonic performance of VSC HVDC," in *Proceedings of the 2020 IEEE Sustainable Power And Energy Conference (iSPEC)*, pp. 982–989, Chengdu, China, November 2020.

[58] Y. Liu and Y. Zhu, "The harmonic characteristics of HVDC system and reduction," in *Proceedings of the 2013 Third International Conference on Intelligent System Design and Engineering Applications*, pp. 1452–1455, Hong Kong, China, January 2013.